www.maajournal.com

Mediterranean Archaeology and Archaeometry
Vol. 21, No 1, (2021), pp. 121-132
Open Access. Online & Print.

DOI: 10.5281/zenodo.4394060

PHYSICOCHEMICAL ANALYSIS OF ORIGINAL AND RESTORED CARBONATE MATERIAL OF THE ROMANIC CHURCH BELL TOWER IN LONGOBUCCO (CALABRIA, ITALY)

A.M. De Francesco*, D. Miriello, D. Forciniti, A. Guido

Department of Biology, Ecology and Earth Sciences, University of Calabria, Via P. Bucci Cubo 15b I-87036 Rende (CS) Italy.

Received: 10/11/2020
Accepted: 11/12/2020
**Corresponding author: A.M.De Francesco (anna_maria.defrancesco@unical.it)*

ABSTRACT

The purpose of this paper is the comparison between the original and restored carbonate material of the bell tower of the Church Matrix in the Longobucco village (Calabria, Italy), built in Romanic style during the XII or XIII century.
The characterization of the original and restored material was performed through micromorphological, petrographic and geochemical approaches utilizing optical and electron microscopy (SEM) observations, X-ray diffraction (XRD), X-ray fluorescence (XRF), mercury porosimetry, and Energy Dispersive Spectroscopy (EDS) analysis. Both materials are composed of low-magnesium calcite with siliciclastic inclusions, more abundant in calcarenites. The main differences are linked to the texture of the two rocks. The very porous continental calcareous tufa is made up of microbialitic boundstones with stromatolitic and thrombolytic-like microfacies. The marine calcarenite is composed of bioclastic grain stones and has a low porosity.
The study shows the importance of the micromorphological and geochemical approach for the characterization of the physical-chemical properties of carbonate materials utilized in restoration and suggest that, for any restoration, the monument and territory history, but also the deeply knowledge of the material is deemed necessary.

KEYWORDS: cultural heritage, restoration; calcareous tufa; calcarenite; Bell Tower; Longobucco; Calabria (Italy).

1. INTRODUCTION

This paper deals with the comparison between the original and restored stone material of the Bell Tower of the Church Matrix at Longobucco (CS), a village located on north-eastern slope of Sila massif (Figs. 1, 2).

The construction of the Romanic monument is datable between the XII and XIII century (Francipane 1938). It is the expression of the Norman-Swabian culture that characterized the policy, society, and economy in the Calabria during the three centuries following the first millennium (De Capua 1997). The monument was probably not conceived in a unique project and it is not functional to the adjacent church. It had the function of warning tower, being placed on the highest area of the medieval village (Adorisio 1983). The structure was erected with a wall lot in which the external layer is made up of square blocks of local calcareous tufa (*sensu* Riding, 1991, and Ford and Pedley, 1996; Figs. 2a, 3). The internal layer, which is composed of riverine blocks, heterogeneous for dimension, shape and lithology, represents the larger part of the masonry section (Forciniti 2005) (Fig. 3).

Figure 1. (A) Panoramic view of the Longobucco village in which is observable the bell tower (red arrow). (B) Historical photo of the the bell tower and Church Matrix.

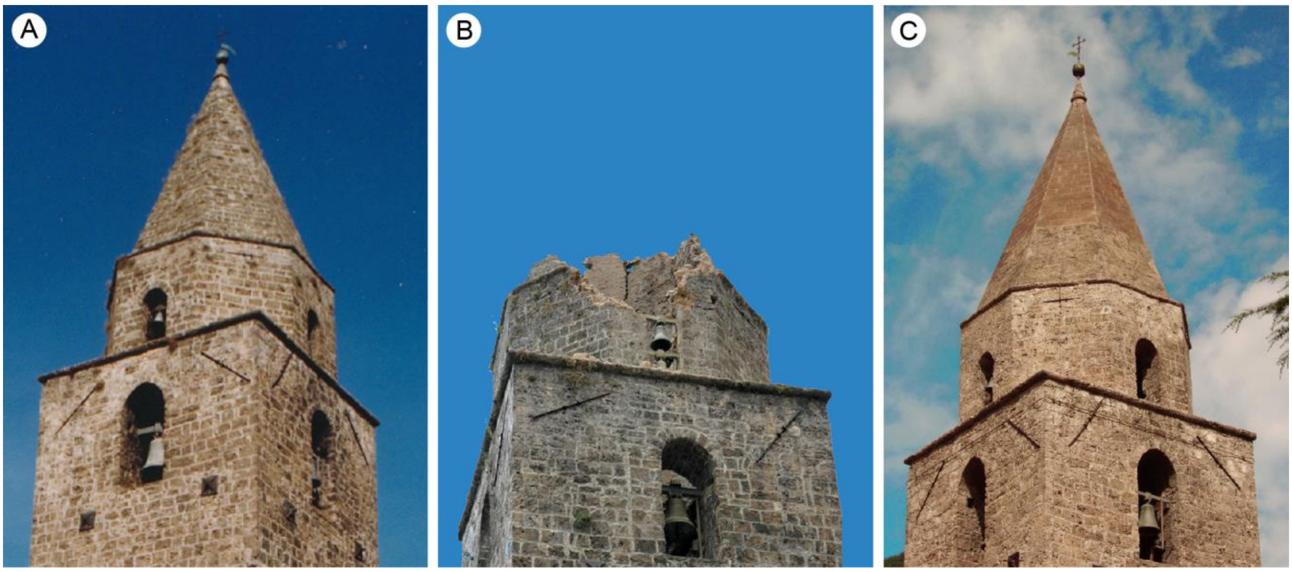

Figure 2. View of upper part of the tower: (A) before and (B) after the destruction; (C) after the restoration.

Figure 3. View of the broken original masonry. Note the wall lot typology of the structure in which the external layer is made up of blocks of local calcareous tufa (black arrow), and the internal layer of riverine blocks (white arrow).

The presence of calcareous tufa is probably the main peculiarity of the monument, considering the rarity of this carbonate in the Calabria Region.

In the night 30th December 2004 a lightning destroyed almost totally the spire and part of the drum in the northern side (Fig. 2B). Soon afterwards the procedures for the consolidation and the restructuration of the building started. The restructuration work ended after about eighteen months: a bioclastic calcarenite of marine origin was used for the reconstruction of the calcareous tufa missing parts (Fig. 4). This material was put in place with a single wall handing masonry and not as a wall lot, like the original structure.

Figure 4. Illustrations of the carbonate material used before (c) and after (a) the restoration. (b) difference between the two materials after the restoration (calcarenite on the left; calcareous tufa on the right).

In this research, the two carbonate rocks, the original calcareous tufa and the replaced calcarenite, were characterized through a multidisciplinary approach aimed to describe and compare: a) the main carbonate component; b) the texture; c) the geochemical characteristics; d) and some physical properties of the two materials. This confirms the importance of the microscopic and chemical characterization for the discrimination of carbonate materials utilized in the restructuration (Hassan and Mahmoud 2021, Salama et al., 2019). In fact, even if carbonate rocks look macroscopically different, their original depositional texture (*in situ* or detrital) and diagenetic state (dissolution, cementation and neomorphic processes) may influence the micromorphological and geochemical parameters making necessary a microscopic and chemical approach for a correct characterization. The restoration of archaeological material must be based not only on the monument and territory history but also on the deeply knowledge of the materials.

2. MATERIALS AND ANALYTICAL TECHNIQUES

The characterization was performed on six representative samples of calcareous tufa, selected from the material collapsed (samples T1-T6), and six samples of calcarenite (samples C1-C6) used for the restoration (Fig. 4). Calcareous tufa is light and soft, with colors (Munsell scale) from light gray (10YR 7/1) to dark gray (10YR 7/2), and from yellow (10YR 7/4, 10YR 8/6, 10YR 7/6) to yellowish brown (10YR 6/4) (Munsell, 1975). Calcarenites are heavier than calcareous tufa, the colors of the fresh sections range from strong brown (7.5YR 5/8; 7.5YR 5/6) to reddish yellow (7.5YR 6/8), to dark brown (7.5YR 4/6).

The samples were described macroscopically, then were analyzed by different analytical methodologies. The thin sections observations with optical polarized microscopy were performed with a Zeiss Axioplan Imaging II under plane and cross-polarized light. They allowed to recognize the carbonate components and siliciclastic grains and to determine the mineralogy, morphology and texture. Mineralogical characterization of the samples was carried out by X-ray diffraction analysis (XRD) on a Philips PW 1710 diffractometer with CuKa radiation operating at 40 Kv and 20 mA. Spectra were taken in the range 5°–60° 2θ and step-times of 1 s/step. Samples were carefully powdered by hand grinding in an agate mortar to produce an average particle smaller than 10 µm. The powder was then side loaded into a glass sample holder. The chemical composition of all samples, in terms of major, minor and trace elements, was determined on pressed powder pellets by X-ray fluorescence spectroscopy (XRF) using a Philips PW 1480 Spectrometer. The following major and trace elements were determined: SiO_2, TiO_2, Al_2O_3, Fe_2O_3 (as total Fe), P_2O_5, MgO, MnO, CaO, Na_2O, K_2O, Ni, Cr, V, La, Ce, Co, Ba, Nb, Zr, Y, Sr and Rb, according to the procedures suggested by Franzini et al. (1972, 1975) and of Leoni and Saitta (1976). Elemental concentrations were quantified using calibration lines up to 70 standard reference materials. Within the range of the measured concentrations, the analytical uncertainties are < 3% for all the components, except for Na_2O, P_2O_5, CaO, TiO_2 and MnO, which may occasionally attain < 10% for very low concentrations.

Micro/nano-morphological studies were carried out with an FEI-Philips ESEM-FEG Quanta 200F Scanning Electron Microscope (SEM) on freshly broken samples, polished surfaces or thin sections. In the last two cases the observed surfaces were prepared with 0.25-micron diamond-impregnated grinding paper, then gently etched (0.05% HCl, 1 min). The samples were then carbon- or gold-coated (ca. 250 Å coating thickness). SEM working conditions were as follows: accelerating voltage of 15kV, working distance between 10 and 15 mm.

The mercury porosimetry analyses have been carried out with Autopore Micromeritics IV 9500 Series.

3. RESULTS AND DISCUSSIONS

Macroscopic Observation

Calcareous tufa – the samples show the typical porous/chalky fabric and peloidal aggregates. Vegetal remains, preserved mainly as casts of fragments and parts of macrophytes or as filaments encased within limpid calcite spar, are abundant (Fig. 4C). The samples are characterized by high primary vacuolation, linked to the original plant framework and growth type (biostructure) (Fig. 4C). The rock did not experience significant compaction phenomena. Calcareous tufa show a complex framework, with tubules lined and encrusted by primary cements, they overlap and cross each other to form bridges that surround and isolate relatively large cavities and vacuoles. The tubule orientation is controlled by the original plant growth way, typical of the fitohermal calcareous tufa (Buccino et al., 1978; D'Argenio et al., 1983; Ferreri 1985; Brancaccio et al., 1986; D'Argenio and Ferreri, 1988; Violante et al., 1994; 1996; Gandin and Capezzuoli, 2008; Capezzuoli et al. 2014).

Calcarenite – this calcareous clastic sedimentary rock, is formed by compaction and cementation of carbonate clasts of size between 0.06 and 2 mm. It also contains a calcareous cementing material that binds the sand grains together and contain a matrix of silt- or clay-size particles that occupy the spaces between the sand grains (Grabau, 1904; Folk, 1959; Dunham, 1962; Pettijohn, 1975). The samples show arenaceous texture with subrounded particles, in which marine fossil fragments are sometimes recognizable (Fig. 4A). The grains are loosely cemented and easily separated by a metal tip. Calcarenite is heavier than calcareous tufa, without evident stratification traces, and with some evidence of transport (iso-oriented grains). The rock shows irregular fractures with uneven and not pulverulent surface, without compaction signals. Easily recognizable are calcite and quartz crystals.

Micromorphological and Petrographic Analyses

Calcareous tufa - The carbonate of the original walls can be classified as "autochthonous calcareous tufa", deriving from "*in situ*" incrustations. Calcareous tufa is the recent denomination of highly porous massive limestone deposited from cool or ambient temperature waters of karstic and/or meteoric derivation, in climate controlled alluvial systems (Pedley, 1990; Ford and Pedley, 1996). It consists of highly porous, poorly bedded, irregularly staked lenticular bodies of massive phytohermal or stromatolitic buildups associated with thin lenticular layers of unsorted phytoclastic sands and/or mud-supported pond-related sediments (Buccino et al., 1978; D'Argenio et al., 1983; Ferreri 1985; Brancaccio et al., 1986; D'Argenio and Ferreri, 1988; Violante et al., 1994; 1996; Gandin and Capezzuoli, 2008). It can be classified as "boundstone", in which the original micrite component is sindepositional lithified (Ferreri 1985). All the samples (T1-T6) show a notably homogeneity. Two microfacies are recognizable (Fig. 5A), stromatolitic-type with typical microlaminations (Fig. 5C), and thrombolytic-type with peloids organized in clots (Fig. 5D).

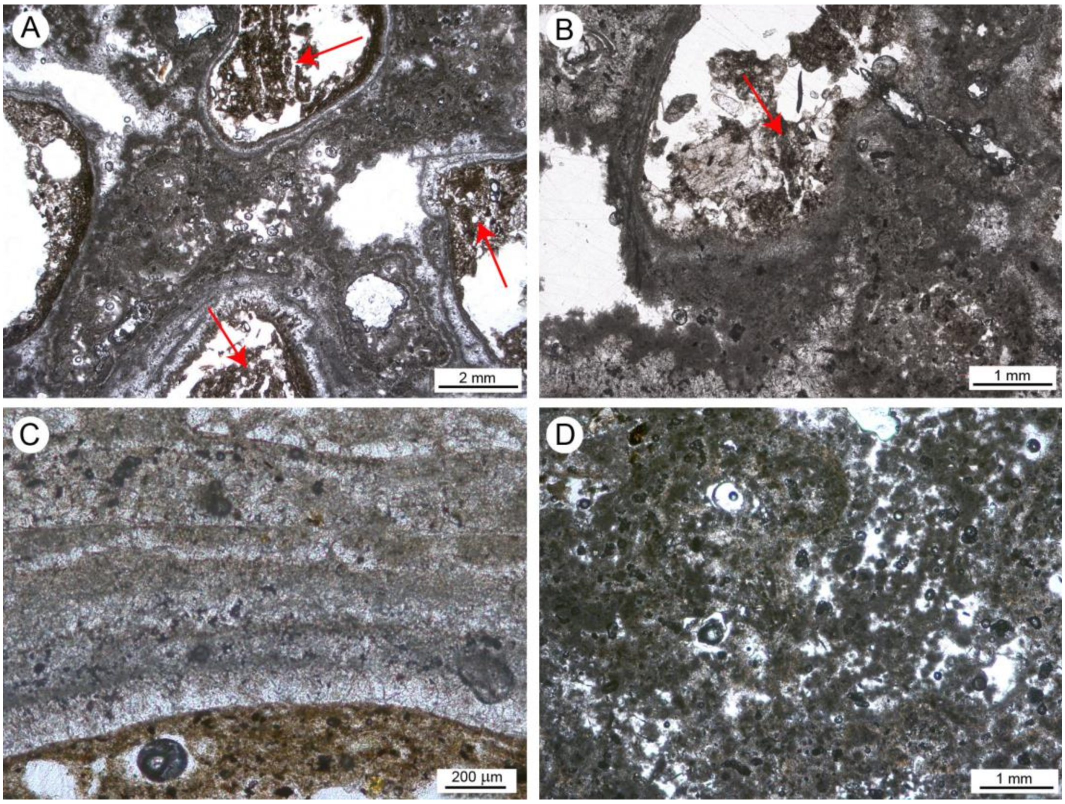

Figure 5. (A, B) Transmitted light photomicrograph of stromatolitic/thrombolitic microfacies characterizing the calcareous tufa; note in the framework cavities the phytoclast remain (red arrows). (C) Stromatolite-type microlaminations characterized by the typical alternation of dark and light laminae. (D) Thrombolytic-type texture with peloids organized in clots.

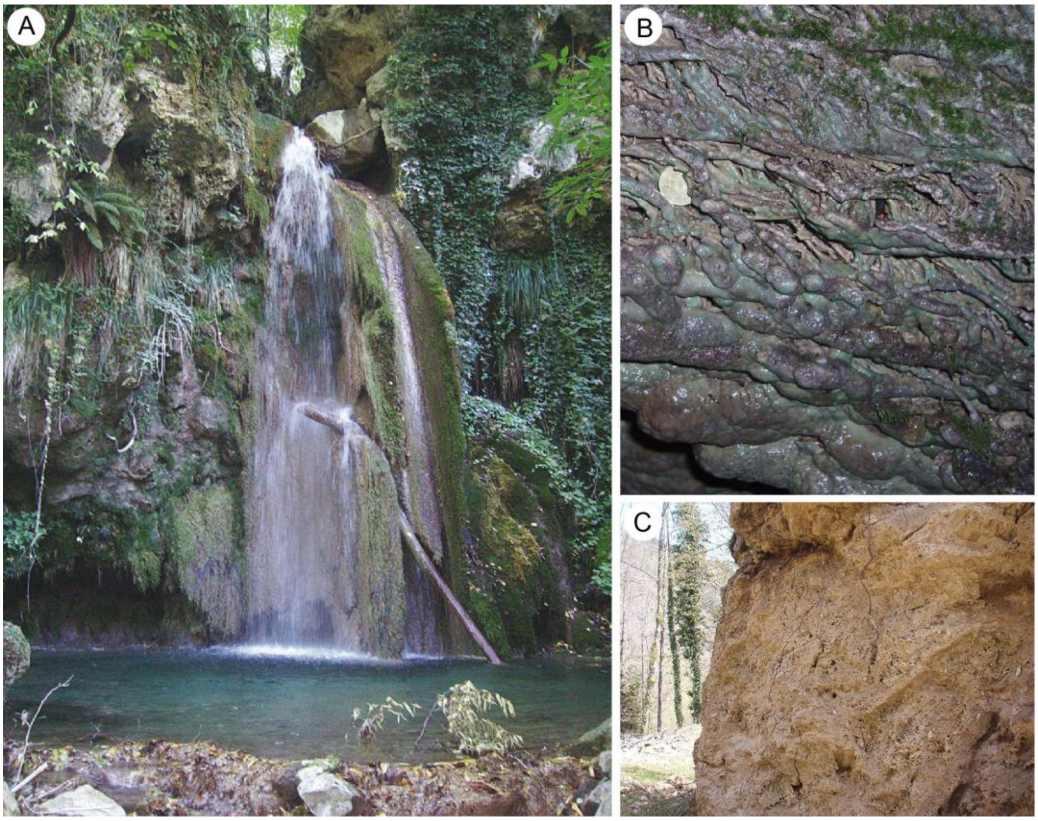

Figure 6. (A) Photo of the calcareous tufa growing up on a pending riverbed in the Vurganera river, near Longobucco village. (B) Detail of the recent phytohermal/microbialite boundstone of the calcareous tufa. (C) Sub-fossil calcareous tufa present along the Vurganera river.

The encrusted phytoclasts are observable as remain of organic matter in the framework cavities (Fig. 6B). Fine siliciclastic components are trapped among the bound stone in all analyzed samples. This fraction indicates a depositional context with very few clay/silt siliciclastic elements, such as pending riverbed. Similar environments, with calcareous tufa deposition, are observable along the Vurganera river near Longobucco Village (Fig. 6 A, B, C).

These recent deposits together with fossil calcareous tufa, observable on the slopes of Avri hill outcrops in Pietra Gna'zzita locality (Fig. 7), allows to hypothesize a local origin of the calcareous tufa utilized to build the bell tower.

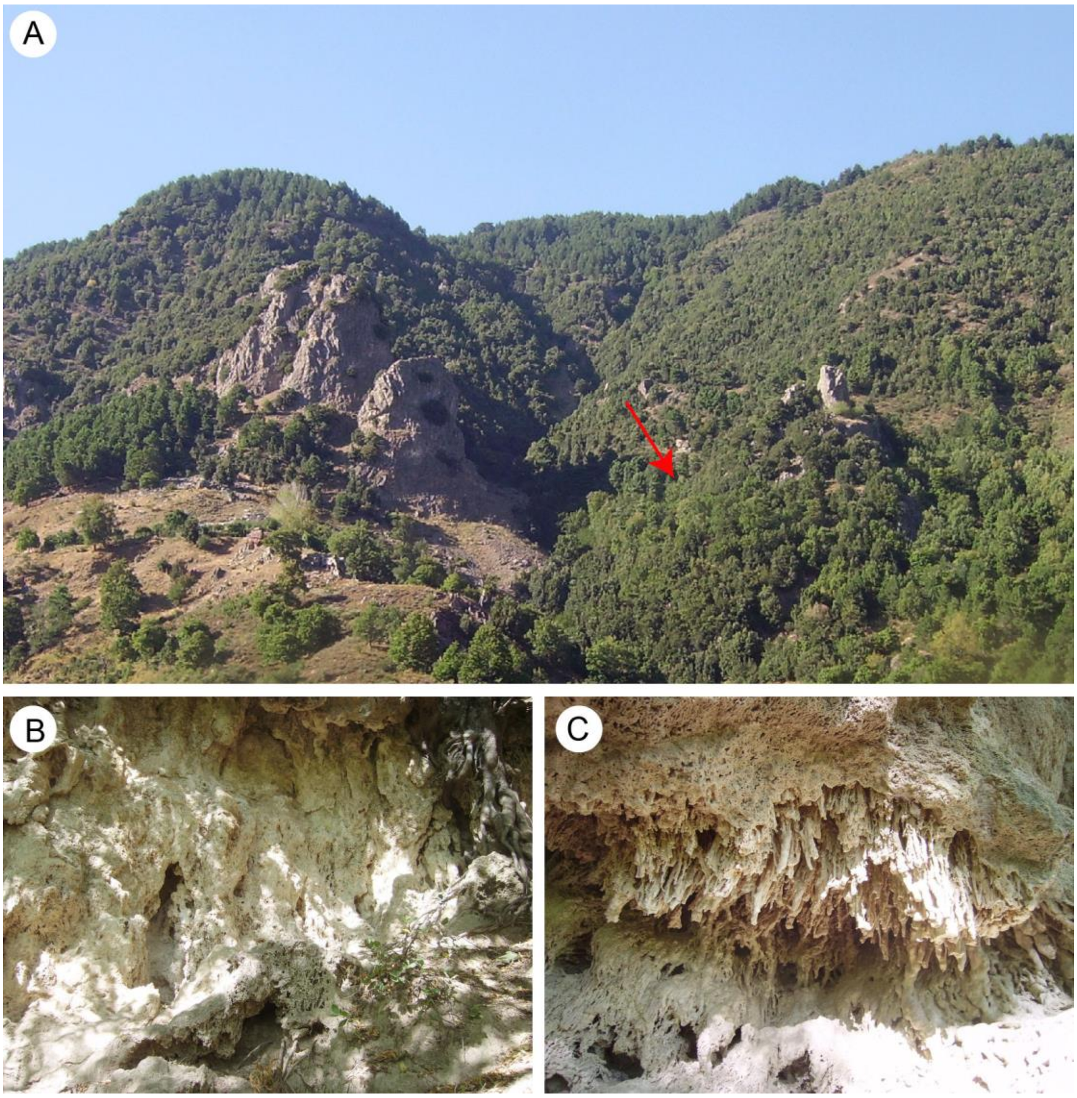

Figure 7. (A) Panoramic view of Pietra Gna'zzita area with the location of the fossil calcareous tufa (red arrow). (B, C) Fossil calcareous tufa showing the characteristics pythohermal/microbialite pattern of growth.

Stromatolitic and thrombolytic fabrics testify the passive role of bacterial communities in supporting the mineralization processes (Figs. 5C, D). Bacterial colonies are commonly found in these systems; they settle in lower-energy microhabitats/niches sheltered from the tractive flow on the bottom of the basins, or on the sides of channels, and passively incorporate carbonate particles in the mucilaginous biofilm (Extracellular Polymeric Substances, EPS) they produce (Merz-Preiss and Riding, 1999; Gandin and Capezzuoli, 2008). Stromatolite-like laminations (Fig. 5C) are characterized by the typical alternation of dark and light laminae, generally parallel/gently bended or wrinkled (Burne and Moore 1987; Riding 1991; Russo et al. 1997; Tucker and Wright 1990). The thrombolyte-like texture (Fig. 5D) are dominated by micritic peloidal clots organized in anti-gravitative fabric, which reflects an induced carbonate precipitation probably by microbial metabolic activity, particularly cyanobacteria and bacteria (Dramis et al. 1999; Russo et al. 1997). The mineralization could have been happened in two phases, the first is correlated to the photosynthetic process producing, around the vegetables, microenvironments supersatured of $CaCO_3$. This phase triggers the deposition of peloidal micrites and it is followed by a second phase in which the carbonate precipitation is led by microbial metabolic activities.

The cavities left by the vegetable decomposition are partially filled by sparry calcite or by siliciclastic debris.

The stromatolitic fabric is affected by neomorphic processes (aggrading diagenesis) which lead an increase of crystal sizes (from few up to tenths of microns). The dark laminae under the optical microscope show crystal sizes less than 10 μm, whereas the light laminae are distinguishable for their larger crystals (Fig. 8A).

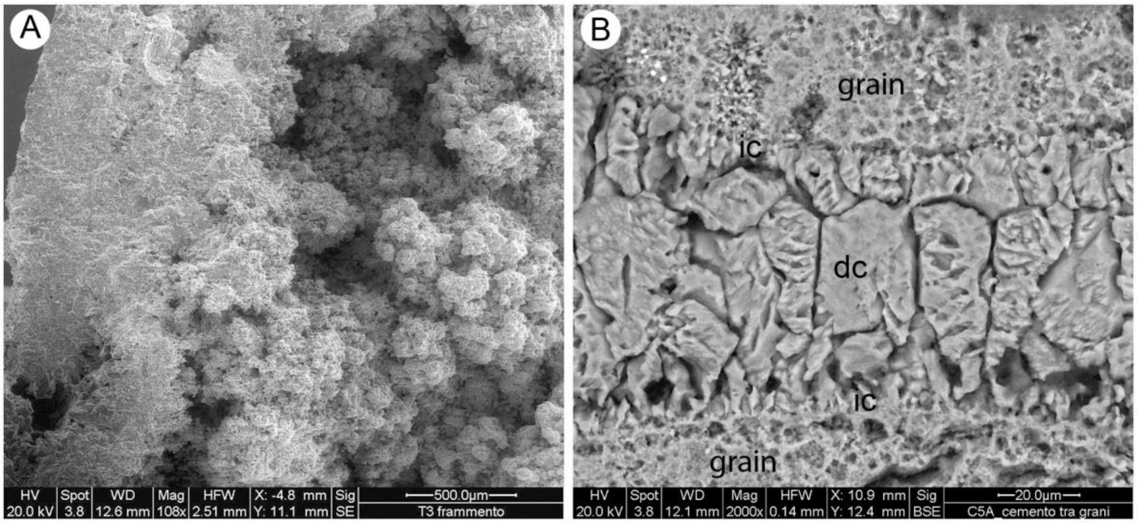

Figure 8. (A) Secondary electrons SEM image of the calcareous tufa showing the typical microbialitic fabrics. On the left the cemented and compact stromatolitic fabric, on the right the loose and porous thrombolytic fabric rich in peloidal clusters. (B) SEM image of calcarenite cements with backscattered electrons. Note the isopachous cements (ic) lining the grains, and the drusy cement (dc) filling the residual cavity.

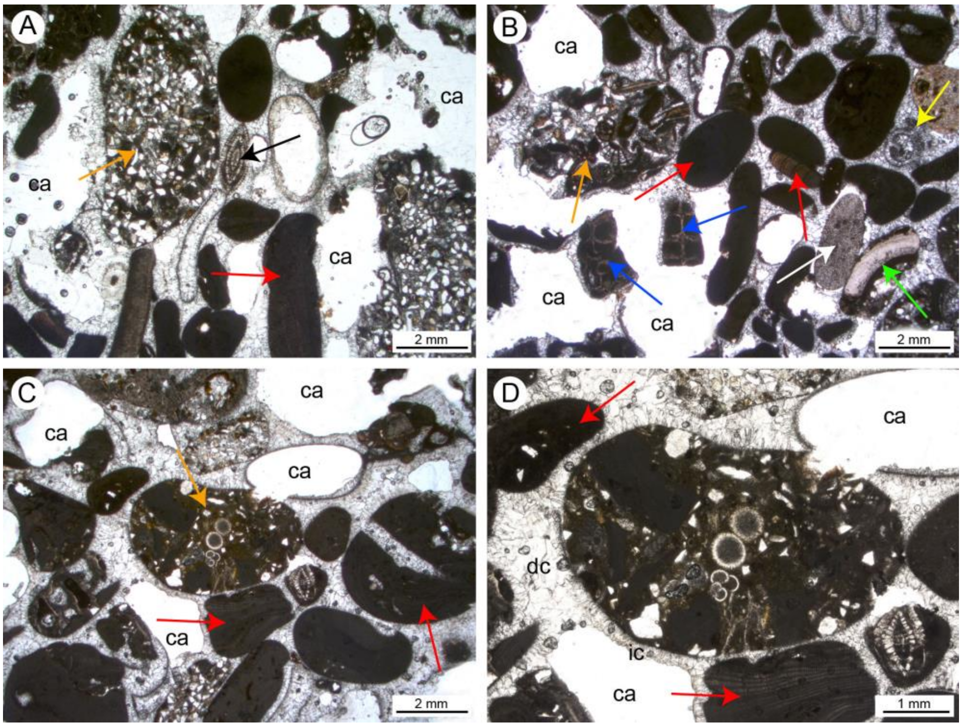

Figure 9. Transmitted light photomicrograph of calcarenite microfacies showing the homogeneity of the texture and composition (A: sample C1; B: sample C3; C: sample C5). The most common skeletal grains are red algae (red arrows), foraminifers (black arrow), gastropods (yellow arrow), bivalves (green arrow), echinoderm plates (white arrow) and bryozoans (blue arrows). Intraclasts are abundant in all the samples (orange arrows). (D) Detail of a well-rounded intraclast. Note the isopachous cements (ic) lining the grains, and the drusy cements (dc) filling the cavities. Cavities are widespread present in all the samples (ca).

Calcarenite (see Fig.9) - The replaced calcarenite is classifiable as grain stone (Dunham 1962). The composition of all the samples (C1-C6) is homogeneous. The grains are mainly composed of intraclasts and skeletal elements, with sub-rounded shapes. The most common skeletal grains are red algae, foraminifers, gastropods, bivalves, echinoderm plates and bryozoans. Fine rounded siliciclastic grains are randomly distributed among the carbonate components (Fig. 9).

The grains are lined with isopachous cements that record the first stage of the diagenesis (marine sindepositional cementation) (Figs. 8, 9). A second phase of diagenesis is represented by drusy cement that reflects deep burial processes (Figs. 8, 9). Both types of cements are calcitic with low magnesium content. Generally, the original cement geochemistry is obliterated by neomorphic phenomena.

The calcarenite characteristics indicate a depositional environment with high hydrodynamic energy. Its secondary porosity may be due to dissolution processes in the last diagenetic phase, characterized by meteoric conditions.

Mineralogical and Chemical Analyses

The difference between the two material is evidenced by the X-Ray diffractometry spectra, which reveals a larger amount of the siliciclastic components in the calcarenites (Table 1).

Table 1. Results of XRD analysis carried out on calcarenites and calcareous tufa samples from Longobucco bell tower. The data are expressed as relative abundances (legend: xxxx = very abundant; xxx = abundant; xx = frequent; x = scarce; - = not detected).

Sample	Calcite	Quartz	Chlorite	Amphibole	Feldspars	K-feldspar
C1	xxxx	xxx	xx	x	x	x
C2	xxxx	xxx	xx	x	xx	-
C3	xxxx	xxx	xx	x	xx	x
C4	xxxx	xxx	xx	x	xx	x
C5	xxxx	xxx	xx	x	xx	x
C6	xxxx	xxx	xx	x	xx	xx
T1	xxxx	x	x	-	-	-
T2	xxxx	x	x	-	x	x
T3	xxxx	x	x	-	x	-
T4	xxxx	x	x	x	-	x
T5	xxxx	x	x	x	x	-
T6	xxxx	x	x	x	-	x

X-Ray diffractometric data show that calcite is the main mineralogical phase in both the studied materials. The main differences are evidenced by the higher amount of quartz, chlorite, amphibole, and feldspars in the calcarenites (Table 1), as testified also by the allochthonous siliciclastic grains observed in optical microscopy. These phases are homogeneously present in all the calcarenite samples while they represent accessory components in the calcareous tufa. Quartz and chlorite are present in low amount in all calcareous tufa samples, amphibole is absent in the samples T1-T3 and feldspars are scantly distributed in all the samples. The low and uneven presence of clay/silt siliciclastic minerals in calcareous tufa is coherent with a pending riverbed deposition.

The results of X-Ray fluorescence on calcareous tufa (T) and calcarenite (C) samples are shown in Table 2. The concentrations are in wt % for major elements and in ppm for trace elements. The data set was recalculated to 100 without L.O.I. values.

The chemical analyses confirm the X-ray diffractometric data. Both the studied sediments have a carbonate composition, with a greater content of $CaCO_3$ in the calcareous tufa. Siliciclastic elements are more abundant in the calcarenites. The X-ray Fluorescence provides an average percentage of calcium oxide (CaO) about 77 % for the calcarenites (C) and 90 % for the calcareous tufas (T) (Tab. 2). Silica, iron, and magnesium oxides contents represent the main discriminant between the two materials. Silica oxides show an average amount of 13.3% in the calcarenites and 5,3% in the calcareous tufa. Iron oxide is present with an average content of 3.1% in the calcarenites and 0.8% in the calcareous tufas. Magnesium oxide is present with an average content of 1,5% in the calcarenites and 0,7% in the calcareous tufa. Sodium, Potassium, Aluminum and Phosphorous oxides are very subordinate in all the samples (Table 2).

Table 2. Analytical results by X Ray Fluorescence of calcarenite (C) and calcareous tufa (T) samples. Concentrations of major element are listed in wt%, trace elements in parts per milion (ppm).

Sample	C1	C2	C3	C4	C5	C6	T1	T2	T3	T4	T5	T6
SiO_2	12,19	13,42	13,20	12,10	13,22	15,77	2,24	6,59	4,75	7,90	1,02	9,27
TiO_2	0,13	0,14	0,14	0,12	0,14	0,21	0,06	0,28	0,09	0,16	0,05	0,17
Al_2O_3	2,18	2,47	2,15	1,82	2,26	4,27	0,45	3,14	0,94	1,51	0,26	1,88
Fe_2O_3	2,84	3,01	2,85	2,65	2,86	4,45	0,27	1,74	0,52	0,84	0,15	1,09
MnO	0,08	0,08	0,08	0,07	0,08	0,10	0,01	0,03	0,02	0,03	0,01	0,02
MgO	1,49	1,42	1,44	1,48	1,54	1,58	0,45	0,73	1,02	0,58	0,89	0,54
CaO	79,12	77,40	78,20	79,81	77,98	71,69	95,07	85,50	91,03	87,31	96,21	85,24
Na_2O	0,31	0,32	0,30	0,35	0,31	0,26	0,20	0,25	0,26	0,23	0,22	0,23
K_2O	0,51	0,60	0,56	0,50	0,57	0,74	0,09	0,77	0,26	0,35	0,04	0,46
P_2O_5	1,17	1,13	1,08	1,09	1,03	0,94	1,17	0,98	1,12	1,10	1,15	1,09
Ni	19	17	22	19	22	26	18	19	17	13	20	22
Cr	10	15	10	13	12	27	10	12	7	4	4	9
V	19	28	28	24	28	45	0	19	0	5	3	8
La	0	0	0	20	0	10	0	0	11	0	12	0
Ce	47	46	46	47	46	87	35	60	51	33	18	65
Co	3	2	4	0	1	2	2	0	0	0	0	0
Ba	89	117	118	149	74	167	135	145	115	127	153	63
Nb	0	0	1	0	1	1	0	0	0	0	0	0
Zr	18	19	24	19	24	25	3	34	10	14	0	18
Y	3	0	1	1	4	7	0	0	0	0	0	0
Sr	277	270	277	283	298	316	201	168	272	198	266	118
Rb	21	24	25	24	25	34	16	33	20	19	14	23

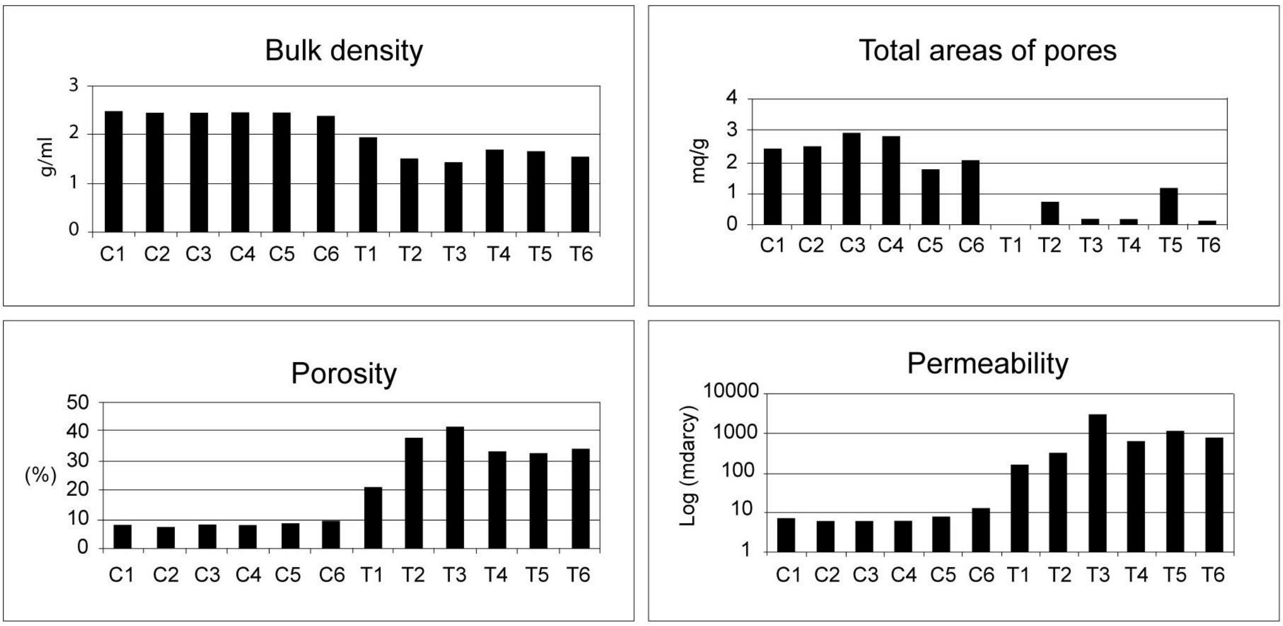

Figure 10. Histograms of porosimetry data showing the difference of the physical parameter between the calcarenite and calcareous tufa.

Mercury Porosimetry Analyses

Several physical parameters, obtained by Mercury Porosimetry analyses, exhibit substantial differences between the two types of rocks (Fig. 10).

The calcarenites show a range of pore diameter from 0,05 to 0,08 μm while the calcareous tufa ranges from 0,67 to 8,16 μm. The average pore diameter of the calcarenite lies between meso- and macropores (not microporous), while the calcareous tufa can be largely classified as a macroporous rock (pore diameter >0.05 μm) (Burne and Moore 1987).

The calcarenites show a range of specific surface (total area of pores) from 1,76 to 2,90 m^2/gr while the calcareous tufa ranges from 0,13 to 1,16 m^2/gr. The skeletal and bulk densities for calcarenite range from 2,43 to 2,50 gr/ml while for calcareous tufa range from 1,45 to 1,99 gr/ml.

The average porosity for calcarenite range from 7,04 to 9,81 % while for calcareous tufa range from 21, to 42%. The permeability for calcarenite range from 6 to 12 millidarcy[1], while it varies from 162 to 2839 millidarcy in the calcareous tufa.

The Mercury Porosimeter analyses denote a substantial homogeneity of the physical parameters among the calcarenite samples in comparison to the calcareous tufa samples. These differences can be linked to the different genetic origin of the two carbonates. Calcarenites form in high hydrodynamic marine depositional systems where the grains suffered transport and sorting processes; the particle are well rounded, and the grain supported texture create a high porous sediment. In the studied calcarenites, the porosity was subsequently reduced by the deposition of primary (isopachous) and secondary (sparry) cements creating a carbonate lithotype with good physical and mechanical properties. The calcareous tufa represents terrestrial and freshwater carbonates; micrites, that precipitate from $CaCO_3$ oversaturated water, encrusts plant remains. In the case of calcareous tufa the framework of the rocks is variable and depend by the type of plants encrusted and position inside the depositional environments. These aspects together with the taphonomy of the organic matter create a high heterogeneity between the materials deriving from the same outcrop. In particular, the analyzed calcareous tufa shows variable physical and mechanical properties, mainly porosity and permeability, linked to the high vacuolar framework due to the decomposition of organic matter and the absence of sparry calcite filling the microcavities.

The different physical properties between the two studied rocks, consequently, affect their behavior towards environmental conditions and therefore on their degradation. In particular, the degradation caused by the formation of ice is greater for rocks with many pores between 3 and 5 μm in size (Siegesmund and Dürrast, 2014).

4. CONCLUSIONS

The analytic study presented in this paper reveal deep physical and chemical differences between the original and restored material of the bell tower "Torre Campanaria" of the Church Matrix at Longobucco village (Calabria, Italy). After the lightning that damaged the bell tower on the night 30th December 2004 a bioclastic calcarenite of marine origin was used for the restoration instead of the original calcareous tufa missing blocks.

The calcareous tufa develops in fluvial systems fed by cool, carbonate-rich waters mainly of karstic and meteoric origin like those forming along Vurganera river near the Longobucco village. The tufa samples are characterized by high porosity, poor organization of the main carbonate components and irregular staked phytohermal/microbialitic structures. Microcrystalline calcite, fine stromatolitic-like texture and peloidal aggregates are the dominant components. This continental rock is of variable color from light gray to dark gray, and from yellow to yellowish brown. The marine calcarenite that was substituted to the damaged calcareous tufa, is heavier and presents arenaceous texture with sub-rounded particles, sometimes constituted by fossil fragments. The grains are loosely cemented. The color ranges from strong brown to reddish yellow, dark brown. The siliciclastic component is relatively higher in calcarenite respect to calcareous tufa.

Considering the different geochemistry, fabric and texture of the two rocks it is likely that they will undergo distinctive weathering ways, making with time unsightly and incongruous the restructuration work.

This multidisciplinary approach can be applied to a broad spectrum of archaeological problematics concerning carbonate materials. In fact, the restoration of archaeological material must be based not only on the monument and territory history but also on the deeply knowledge of the material.

[1] darcy (or darcy unit) and millidarcy (md or mD) are units of permeability, named after Henry Darcy. They are not SI units, but they are widely used in petroleum engineering and geology. Like some other measures of permeability, a darcy has dimensional units in length[2].

ACKNOWLEDGEMENTS

The authors wish to express their gratitude to the Editor and two anonymous reviewers for their constructive comments that greatly improved the paper. This research was financially supported by MIUR (ex 60% 2019 A. De Francesco, University of Calabria).

REFERENCES

Adorisio, A.M. (1983) Il campanile di Longobucco. *Rivista "Calabria Sconosciuta"*, 24, Reggio Calabria (Italy).

Brancaccio, L., D'Argenio, B., Ferreri, V., Preite Martinez, M., Stanzione, D., Turi, B. (1986) Caratteri tessiturali e geochimica dei travertini di Rocchetta a Volturo (Molise). *Bollettino della Società Geologica Italiana*, Vol. 105, pp. 265-277.

Buccino, G., D'Argenio, B., Ferreri, V., Brancaccio, L., Ferreri, M., Panichi, C., Stanzione, D. (1978) I travertini della bassa Val Tanagro (Campania): studio geomorfologico, sedimentologico e geochimico. *Bollettino della Società Geologica Italiana,* Vol. 97, pp. 617-646.

Burne, R.V. and Moore, L.S. (1987) Microbialites: Organosedimentary deposits of benthic communities". *Palaios,* Vol. 2, pp. 241-254.

D'Argenio, B., Ferreri, V., Stanzione, D., Brancaccio, L., Ferreri, M. (1983) I travertini di Pontecagnano (Campania): geomorfologia, sedimentologia, geochimica. *Bollettino della Società Geologica Italiana*, Vol.102, pp. 123-136.

D'Argenio, B. and Ferreri, V. (1988) Ambienti deposizionali e litofacies dei travertini quaternari dell'Italia centro-meridionale. *Memorie della Società Geologica Italiana*, Vol.41, pp. 861-868.

Capezzuoli, E., Gandin, A., Pedley, M. (2014) Decoding tufa and travertine (fresh water carbonates) in the sedimentary record: The state of the art. *Sedimentology,* Vol. 61, No. 4, pp. 1–21.

Dramis, F., Materazzi, M., Cilla, G. (1999) Influence of Climatic Changes on Freshwater Travertine: a new hypothesis. *Physics and Chemistry of the Earth*, Vol. 24, No. 10, pp. 893-897

De Capua, G. (1997) *Longobucco dalle origini al tempo presente*. Studio Zeta Ed., Rossano (CS), Italy.

Dunham, R.J. (1962) Classification of carbonate rocks according to depositional texture. Ham, W.E. (Ed.), Classification of carbonate rocks, *American Association of Petroleum Geologists Memoir* 1, pp. 108-121.

Ferreri, V. (1985) Criteri di analisi di facies e classificazione dei travertini pleistocenici dell'Italia meridionale. *Rendiconti Accademia di Scienze Fisiche e Matematiche*, 52, Napoli, pp. 1-47.

Folk, R.L. (1959) Practical petrographic classification of limestones. *American Association Petroleum Geologists Bulletin*, Vol. 43, pp. 1–38.

Forciniti, D. (2005) *Il campanile della Chiesa Matrice di Longobucco (CS): studio comparativo tra il travertino originario e la calcarenite utilizzata nel restauro*. Unpublished master's thesis, Department of Earth Sciences. University of Calabria, Italy.

Ford, T.D. and Pedley, H.M. (1996) A review of tufa and travertine deposits of the world. *Earth Science Revue*, Vol. 41, pp. 117-175.

Francipane, A. (1938) *Elenco degli edifici monumentali, LVIII-LX, Catanzaro-Cosenza-Reggio Calabria.* Ministero dell'Educazione Nazionale, Roma.

Franzini, M., Leoni, L., Saitta, M. (1972) A simple method to evaluate the matrix effects in X-ray fluorescence analysis. *X-ray Spectrometry*, Vol. 1, pp. 151–4.

Franzini, M., Leoni, L., Saitta, M. (1975) Revisione di una metodologia analitica per fluorescenza X basata sulla correzione completa degli effetti di matrice. *Rendiconti della Società Italiana di Mineralogia e Petrologia*, Vol. 31, pp. 365–78.

Gandin, A. and Capezzuoli, E. (2008) Travertine versus calcareous tufa: distinctive petrologic features and stable isotopes signatures. *Italian Journal of Quaternary Science*, Vol. 21, pp. 125-136.

Grabau, A.W. (1904) On the classification of sedimentary rocks. *American Geologist,* Vol. 33, pp. 228–247.

Hassan S.A. Mahmoud (2021) Multiscientific approach for the characterization and assessment of the degradation state of the historical al-shafi'i mosque walls (jeddah, kingdom of saudi arabia). *Scientific Culture*, Vol. 7, No. 1, pp. 1-19. DOI: 10.5281/zenodo.4107161.

Leoni, L. and Saitta, M. (1976) X-ray fluorescence analysis of 29 trace elements in rocks and mineral standards. *Rendiconti della Società Italiana di Mineralogia e Petrologia*, Vol. 32, pp. 497–510.

Merz-Preiss, M, and Riding, R. (1999) Cyanobacterial tufa calcification in two freshwater streams: ambient environment, chemical thresholds and biological processes. *Sedimentary Geology*, Vol. 126, No.1-4, pp. 103-124.

Munsell Soil Color Charts (2000) Gretagmacbeth, New Windsor, NY.

Pedley, H.M. (1990) Classification and environmental models of cool freshwater tufas. *Sedimentary Geology*, Vol. 68, pp. 143-154.

Pettijohn, F.J. (1975), Sedimentary Rocks, 3rd Harper and Row, New York.

Riding, R. (1991) Classification of microbial carbonates. Riding, R, (Ed.), *Calcareous Algae and Stromatolites,* Springer-Verlag, Berlin, pp. 21-51.

Russo, F., Neri, C., Mastandrea, A., Baracca, A. (1997) The Mud Mound Nature of the Cassian Platform Margins of the Dolomites. A case History: The Cipit Boulders from Punta Grohmann (Sasso Piatto Massif, Northern Italy). *Facies,* Vol. 36, pp. 25-36.

Siegesmund, S., H. Dürrast (2014) *Physical and mechanical properties of rocks. In: stone in architecture. properties, durability*, Siegesmund.S.S and Snethlage.R (eds), 107–20. 5th ed. Springer, Berlin, Germany.

Salama, K, Mona F.Ali, Said M. El-Sheikh (2019) A comparison between nano calcium carbonate, natural calcium carbonate and converted calcium hydroxide for consolidation. *Scientific Culture*, Vol. 5, No. 3, pp. 35-40. DOI: 10.5281/zenodo.3340107.

Tucker, M.E. and Wright, V.P. (1990*) Carbonate Sedimentology*. Oxford: Blackwell Science.

Violante, C., Ferreri, V., D'Argenio, B. (1996) Modificazioni geomorfiche controllate dalla deposizione di travertino. *Il Quaternario Italian Journal of Quaternary Sciences*, Vol. 9, No. 1, pp. 213-216.

Violante, C., Ferreri, V., D'Argenio, B., Golubic, S. (1994) Quaternary travertines at Rocchetta a Volturno (Isernia, Central Italy). Facies analysis and sedimentary model of an organogenic carbonate system. *I.A.S. 15th Regional Meeting,* April 1994, Ischia, Guide book to the field trip, pp. 3-23.